Communications

Elastic Registration for Retinal Images Based on Reconstructed Vascular Trees

Bin Fang* and Yuan Yan Tang

***Abstract*—The vascular tree of the retina is likely the most representative and stable feature for eye fundus images in registration. Based on the reconstructed vascular tree, we propose an elastic matching algorithm to register pairs of fundus images. The identified vessels are thinned and approximated using short line segments of equal length that results a set of elements. The set of elements corresponding to one vascular tree are elastically deformed to optimally match the set of elements of another vascular tree, with the guide of an energy function to finally establish pixel relationship between both vascular trees. The mapped positions of pixels in the transformed retinal image are computed to be the sum of their original locations and corresponding displacement vectors. For the purpose of performance comparison, a weak affine model based fast chamfer matching technique is proposed and implemented. Experiment results validated the effectiveness of the elastic matching algorithm and its advantage over the weak affine model for registration of retinal fundus images.**

***Index Terms*—Elastic matching, fast chafer matching, retinal image registration, vascular tree.**

I. Introduction

Temporal registration is perhaps one of the most significant applications in the diabetic retinopathy screening program [1]. Typically, a patient is required to have his/her retinal fundus photographs taken over a fixed time interval. By comparing the different photographs, physicians are able to evaluate the progress of retinal diseases.

The registration of eye fundus images is a nontrivial task [2]. The anatomy of the human eye with its sphere-like shape and physical properties of optical imaging system leads to the quadratic model and stereo registration [3], [4]. However, the fact that visible surface of the retina is roughly planar in the images suggests that a weak affine model may be sufficient without losing too much accuracy. As a result, much work in retinal image registration uses the weak affine transformation model and employs detected vessel features. In terms of the image contents involved, various approaches are classified into either segmentation-based techniques focusing on aligning the extracted features of the image subjects or pixel property-based techniques using the full image content for alignment. The major drawback of the pixel based techniques is that they are unable to deal with the total surface of eye fundus images [5]. Zana [6] reported a Bayesian Hough transform based method to determine the best weak affine transformation coefficients. Heneghan [3] used an expectation-maximization (EM) algorithm to identify matched pairs of control points. Can [4] used a similarity-weighted histogram technique to search correspondence of control points. Pinz [7] used Powell's method while Peli [8] employed an exhaustive search technique to find the best transformation parameters. The problem is that it is difficult to sort out the optimal parameters when initial seed points are insufficient. To employ a large number of initial seeds incur expensive computation load which takes the risk of impractical implementation.

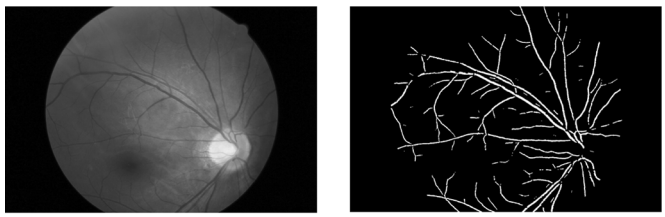

(a) (b)

Fig. 1. (a) Original grey-level retinal fundus image, and (b) reconstructed vascular tree.

In this paper, we propose the use of an elastic matching algorithm which is similar to that in [9] for retina registration without heavy calculation of sorting out the optimal transformation of the parametric models. Vascular trees feature of retinal fundus image are reconstructed using a method we proposed before [10] and are represented by a set of elements of straight short line segments with equal length. An elaborately designed energy function is employed to guide the deformation of the transformed vascular tree to optimally match a reference vascular tree. Mapped positions of pixels in the transformed retinal image are computed using displacement vectors of feature points which are able to be conveniently determined by the matching list at the end of elastic matching process. In order to compare registration performance, a weak affine model based fast chamfer matching technique is proposed and implemented. Our experiments demonstrate the effectiveness of the proposed elastic matching algorithm and advantage over the weak affine model for temporal registration of retinal fundus images. Internal relationship between overlap and center error and computation cost are investigated.

II. Methods

A. Vascular Tree Reconstruction

We have proposed a robust method [10] to effectively reconstruct the vascular tree and the results are to be employed as the features for our registration algorithms in this work. The technique is briefly explained as follows. Vessels are enhanced by mathematic morphological transformation and evaluation of curvature of the vessel-like patterns is performed. Then, a set of morphological filters are applied to segment vessel objects. In order to recover the complete vascular tree, a reconstruction process is performed based on dynamic local region growing. Fig. 1 shows the reconstructed vascular tree for an entire retina.

B. Elastic Matching Algorithm

Parameter transformation model based registration suffers from the difficulty of finding the optimal model parameters. An attempt in nonparametric approach for retinal image registration was reported by Jasiobedzki [11]. The problem of the active contours is that they seem to be attracted only to features that they are initially close to. To cope with

Manuscript received May 14, 2004; revised July 4, 2005. *Asterisk indicates corresponding author*.

*B. Fang is with the Department of Computer Science, Chongqing University, Chongqing 400044, P.R. China.

Y. Y. Tang is with the Department of Computer Science, Chongqing University, Chongqing 400044, P.R. China. He is also with the Department of Computer Science, Hong Kong Baptist University.

Digital Object Identifier 10.1109/TBME.2005.863927

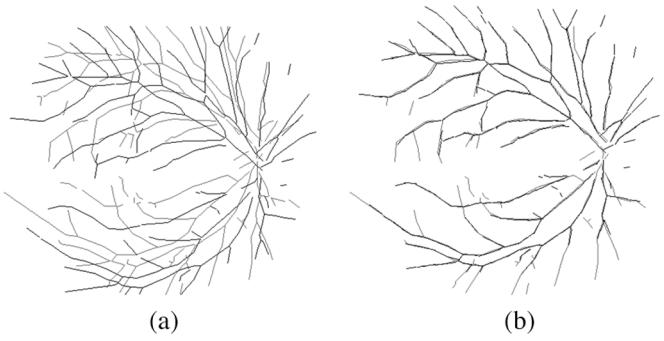

Fig. 2. (a) Overlapped image of the *Template* vascular tree (black lines) and the *Input* vascular tree (grey lines) before matching and (b) overlapped image of the vascular trees after matching.

the complex structure of vascular trees, we propose the use of elastic matching for retina registration without searching optimal model parameters.

The aim of the elastic matching algorithm is to elastically deform a set of elements of one vascular tree in order to match the corresponding elements of another vascular tree. An energy function is designed to guide the movement of elements which enables to correctly align two sets of elements both globally and locally.

Let the *Template* pattern and *Input* pattern be the two binary vascular trees to be registered. Thinning is performed so that the resulting patterns consist of lines and curves with one pixel wide only. Each resulting straight line is then divided up into smaller segments of approximately equal lengths referred as an "element" which is represented by its slope and the position vector of its midpoint.

The *Template* is elastically deformed in order to match with the *Input*. The process consists of overlaying one pattern on top of the other, and the set of *Template* elements are iteratively moved until the corresponding elements of both *Template* and *Input* patterns meet, as illustrated in Fig. 2. The objective is to achieve maximum similarity between the resulting patterns while minimizing the deformation. This is achieved through the minimization of an energy (or cost) function which is similar to that in [9]. The energy function E_1 used to guide the movements of the *Template* elements toward the *Input* elements is defined as follows:

$$E_1 = -K_1^2 \sum_{i=1}^{N_I} \ln \sum_{j=1}^{N_T} \exp\left(-\frac{|\mathbf{T}_j - \mathbf{I}_i|^2}{2K_1^2}\right) f(\theta_{Tj,Ii}) + \sum_{j=1}^{N_T}\sum_{k=1}^{N_T} w_{jk}\left(d_{Tj,Tk} - d^0_{Tj,Tk}\right)^2. \quad (1)$$

For detail information of involved parameters, refer to [9].

The movement $\Delta\mathbf{T}_\mathrm{j}$ applied to $\mathbf{T}_\mathrm{j}$ is equal to $-\partial \mathrm{E}_1/\partial\mathbf{T}_\mathrm{j}$ and is given by

$$\Delta T_j = \sum_{i=1}^{N_I} u_{ij}(\mathbf{I}_i - \mathbf{T}_j) + 2\sum_{m=1}^{N_T}(w_{mj} + w_{jm}) \times \left[\left(\mathbf{T}_m - \mathbf{T}^0_m\right) - \left(\mathbf{T}_j - \mathbf{T}^0_j\right)\right] \quad (2)$$

where

$$u_{ij} = \frac{\exp\left(-\frac{|\mathbf{I}_i - \mathbf{T}_j|^2}{2K_1^2}\right) f(\theta_{Ii,Tj})}{\sum_{n=1}^{N_T} \exp\left(-\frac{|\mathbf{I}_i - \mathbf{T}_n|^2}{2K_1^2}\right) f(\theta_{Ii,Tn})}$$

and $\mathbf{T}^0_\mathrm{j} = \text{initial value of } \mathbf{T}_\mathrm{j}$

One major advantage of using the designed energy function is that each *Template* element normally does not move toward its nearest *Input* element but tends to follow the weighted mean movement of its neighbors in order to minimize the distortions within the neighborhood during first several iterations of the matching process so that global alignment can be achieved. At the end of the iterations, the corresponding parts of the two vascular trees should hopefully be the nearest to each other locally, as shown in Fig. 2(b).

We define feature points of an element being the middle and end points of the elements we used in the elastic matching method. Once having identified correspondence of each feature point between two vascular trees, we are able to calculate displacement vectors for feature points of the *Template* by referring to feature pixel locations in the *Template* and the matched pixel locations in the *Input* as follows:

$$\mathbf{P}_j = \mathbf{T}_j - \mathbf{I}_{i(j)} \quad (3)$$

where $\mathbf{T}_\mathrm{j}$ is the location of feature point j in the *Template* and $\mathbf{I}_{\mathrm{i(j)}}$ is the location of the feature point of *Input* which is matched to j.

In order to determine the mapped position of pixels in the *Template* retinal images, we need to first compute the displacement vector for each pixel. Considering the nonlinear characteristics of the elastic matching algorithm, we define the displacement vector as follows:

$$\Delta M = \sum_{j=1}^{N} w_j \mathbf{P}_j. \quad (4)$$

N is the size parameter of the Gaussian window which establishes neighborhood of correlation, w_j are the correlation weights in the Gaussian correlation window where $w_j = \exp(-(j-1)^2/(2\times N^2))$ and $j = 1, 2, \ldots, \mathrm{N}$. $\mathbf{P}_j$ is the displacement vector of feature point j of the *Template* in the Gaussian window sorted in the order of increasing distance from that pixel. It is obvious that the mapped positions of pixels in the *Template* retinal image are able to be conveniently calculated as the sum of their original positions and corresponding displacement vectors. If at the mapped location there is only one original pixel of the *Template* involved, the grey-level of the transformed pixel keeps as its original value. When the case is that more than two pixels of the *Template* mapped to one new transformed location, the grey-level is set as the arithmetic average of grey-levels of all pixels involved.

C. Weak Affine Model Based Fast Chamfer Matching

To compare performance of the elastic matching algorithm, we adopt the weak affine model of translations and rotation for globally matching two vascular trees of retinal fundus images. The model can be mathematically expressed as follows:

$$\begin{bmatrix} x' \\ y' \end{bmatrix} = \begin{bmatrix} \cos\theta & -\sin\theta \\ \sin\theta & \cos\theta \end{bmatrix} \begin{bmatrix} x \\ y \end{bmatrix} + \begin{bmatrix} \Delta x \\ \Delta y \end{bmatrix}. \quad (5)$$

We employ the idea of fast chafer matching [12] which follows a multiresolution strategy to sort out optimal estimations of model parameters with the aim of reducing computation load. This method involves iterative calculation of the registration from coarse derivation of the image up to the image itself by using sorted seeds at lower resolution as initial seeds at higher resolution. A large number of seeds scattering in parameter space at the coarse level (lower resolution) can be investigated and most of these seeds could be readily rejected. The method is briefly described as follows.

The original image is at the highest resolution, finest level (level 0). To create lower resolution image at coarse levels, each block of four pixels of the original image is represented by one pixel in the previous level image. The start resolution (level N) is decided by whether the object in an image is recognizable.

One vascular tree to be matched is called the *Template* and the other the *Input*. A sequential distance transformation [12] is applied to create *Input* distance map. The *Template* is superimposed on the *Input* distance map. The measurement of goodness of match is in the form of a distance function which is defined as the squares of the pixel values of *Input* distance map that the *Template* hits. It is obvious that a perfect fit will result in a minimum value of the distance function. Local transformations with distances larger than a threshold are rejected and only those with smaller distances are used as initial seeds of transformation parameters for matching two vascular tree features in the next finer resolution level. When the search at the zero level (original image) is completed, the transformation with smallest distances determines the optimal model parameters. Hence, the mapped positions of pixels in the *Template* retinal fundus image are ready to be uniquely identified according to the determined optimal transformation model.

III. Results

A. Pre-Processing and Initialization of Transformation Models

The image database that we use to evaluate performance of the proposed registration algorithms consists of 47 grey-level fundus images from eleven patients at different time period. All fundus images were acquired using a digital fundus camera applied directly to the fundus microscope. The image size was 512 × 512. Spatial resolution was 7.141 $\mu\mathrm{m/pixel}$. We pair the 47 fundus images in different order to obtain a total of 128 pairs. The vascular trees were first reconstructed by the method explained in Section II. Next, vascular trees were thinned to be one-pixel wide skeletons to be ready as features for registration.

In the elastic matching algorithm, each line or curve is approximated by fitting a sequence of short straight lines ("elements") of about 20 pixels long. This length of 20 pixels is chosen according to the size of the image and it is not crucial in the registration procedure. It is obvious that if the element is too short, it will result in many elements. The possibility of matching failure would rise and the computational complexity for matching would be high. On the other hand, if each element was too long, the resolution of the representation would be low and the matching of local details would be affected.

The neighborhood size parameters K_1 and K_2 should be large initially to allow large distortion of the two patterns being matched, and the parameters should be successively decreased to allow finer and finer alignment. This procedure was adopted to alleviate the local minimum problem associated with gradient descent procedures. In the experiments, to allow two different vascular trees with large translation to be registered, both K_1 and K_2 were set to 90 pixels to start with. After each set of 10 iterations, K_1 and K_2 were updated as follows:

$$\mathrm{K}_1 := \mathrm{K}_1 - \max(0.1, 0.05 * \mathrm{K}_1) \tag{6}$$

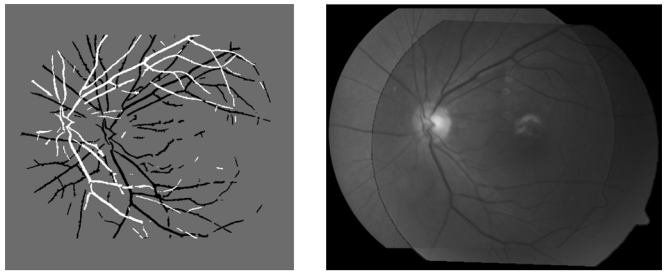

(a) (b)

Fig. 3. (a) Overlapped extracted vascular trees, (b) fused image. Overlap is 79% and centreline error for FCM is 1.94 and 1.67 for EM.

$$\mathrm{K}_2 := \mathrm{K}_2 - \max(0.1, 0.01 * \mathrm{K}_2). \tag{7}$$

The process stopped when K_1 was reduced to below 1.0 pixel. K_2 was scheduled to decrease at a lower rate than K_1 because it was found that if they decrease at the same rate, the distortion would be quite large during the last few iterations. Hence K_2 decreased at a slower rate to allow for more neighboring elements influencing each other in order to minimize the deformation in the local structure.

In the registration using the weak affine transformation model, the depth of multiresolution in the fast chamfer matching method is set to 4, resulting in the size of the fourth-level images being 32 × 32. 54 initial positions were attempted at the lowest resolution, namely: 3 × 3 translation points, separated by 3 pixels, and 6 equidistant rotation angles. The total number of seeds would be increased to 150 when registration using the previous selected 54 seeds was unsuccessful where 5 × 5 translation points and 6 equidistant rotation angles were tested.

B. Performance of the Elastic Matching Algorithm

Visual assessment has been widely adopted to qualify the registration results in two ways. One way is to produce a checkerboard of reference and registered images [5] while the other to superpose transformed vascular tree of the registered image on those of the reference image [6]. In this paper, we not only give superposed images of two vascular trees to be registered, we also present composite images of fused reference and registered images for a better view of the registration. Overlapped portion of the fused image between the reference and registered images is obtained through the implementation of a classical greyscale image fusion method with average strategy [13]. The fast chamfer matching method is referred to as FCM, and the elastic matching algorithm is replaced by EM in the following explanations. A successful registration example is shown in Fig. 3.

Visual evaluation is useful to provide convenience for judging success of registration. However, it may not be sufficient to compare the registration quality for different matching strategies such as those used in this study. Quantitative criterion has to be developed for the purpose to evaluate registration accuracy and effectiveness. We follow the definition of registration error to be the centreline error proposed by Can [4]. Another important index to be taken into account is the percentage of overlap between the reference image and the registered image. It is defined as the fraction of the registered image appearing in the reference image.

The average centreline errors and running times of successful registration of 121 image pairs for both methods are given in Table I. Average centreline error for the EM algorithm is 2.06 pixels with standard deviation equal to 0.98 pixels while FCM method has 2.19 pixels centreline error and 1.14 pixels standard deviation. The average time taken for EM is 69.00 s and 83.89 s for FCM when both methods are implemented on a Pentium III 866. The results indicate that the elastic

TABLE I
COMPUTATION COMPLEXITY AND PERFORMANCE FOR EM AND FCM (54 SEEDS)

Methods	Pairs of images	Average centreline error (pixels)	Standard deviation (pixels)	Average time taken (s)
FCM	121	2.19	1.14	83.89
EM	121	2.06	0.98	69.00

matching algorithm is able to efficiently achieve comparable registration performance of the weak affine model. The calculation cost depends on the complexity of the extracted vascular trees. If the number of vessels appearing in the extracted vascular trees is relatively large, the calculation load involved for the distance and the displacement vector updates will be heavier. However, all registration can be done in a few minutes for both FCM and EM. The longest time for EM to register an image pair is 150 s and 197 s for FCM.

In order to investigate possible internal relationship between images overlap and measured centerline errors, a plot of the centerline error against the percentage of overlap between image pairs is shown in Fig. 4. Fig. 4(a) shows the scatter plot of the centreline errors for 121 pairs of images that are successfully registered using EM and FCM with 54 seeds and Fig. 4(b) shows the average errors in 10 percent range from 60–70 to 90–100. It is clear that although centreline error decreases as overlap increases, the trend is not obvious. Successful registration may have centreline error of 4.97 pixels and the smallest centreline error is 0.63. This phenomenon can be explained that although median statistics of centreline error are used to alleviate error measure from missing or spurious centrelines, the effects on measuring centreline error of vessels in registered image that do not appear in retina area of the reference still exist, and this difference in extracted vascular trees is mainly related to the vessel detection process. Hence, it has lost the comparison foundation to other works [4], [14] by examining the centreline error used here. An accurate measurement of registration accuracy will be investigated in the future study. In addition, for those pixels on the transformed vascular tree other than the feature points, the displacement vectors involved to determine pixel mapped positions are not computed directly using the matching list like the feature points but according to (4) which may incur inaccurate alignment.

In addition, there are five cases in this study where the FCM method uses 54 initial seeds to search for the global minimization of the distance function but is unable to successfully register image pairs. On the other hand, the EM algorithm can still achieve successful registration. Although best transformation parameters were estimated by FCM when the total number of seeds has been increased to 150 where 5×5 translation points and 6 equidistant rotation angles were tested, this is achieved at a significant increment in the processing time, see Table II. Processing time for FCM is triple that of EM. In spite of that, there are still two cases where FCM fails to register image pairs even when 150 initial seeds were used. For the EM method, although there were a few vessels not aligned properly, majority of the vascular structures is successfully matched. These results demonstrate the advantage of the proposed elastic matching algorithm in efficiency with less runtime and effectiveness of successful registration for special cases than the FCM method.

IV. CONCLUSION

In this paper, we have described an elastic matching algorithm based on reconstructed vascular trees for temporal registration of pairs of eye fundus images. Registration methods employing weak affine model have to estimate optimal model parameters by means of searching global minimization of designed functions relative to similarity measurement. The problem is that it is often difficulty to conveniently obtain optimal parameters estimation with small size of initial seeds set. Increasing the number of initial seeds incurs heavy computation load and even does not guarantee successful registration. On the other hand, the proposed elastic matching algorithm is able to achieve both global and local alignments avoiding heavy calculation. Experiment results show that the elastic matching algorithm performs comparably in both accuracy and efficiency to that of the weak affine

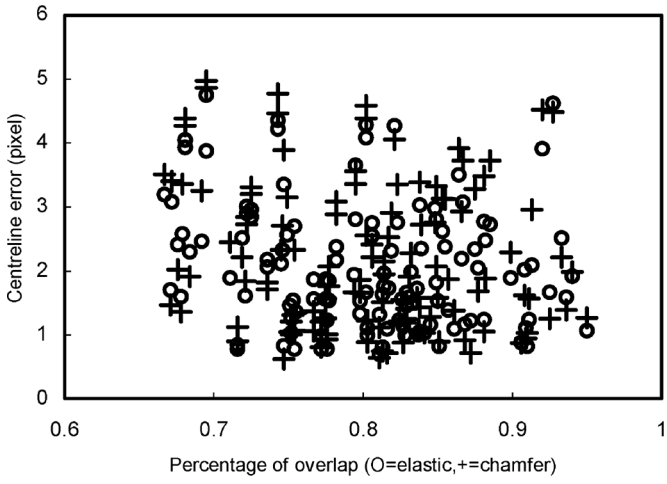

Fig. 4. Overlap versus centreline errors. (a) Scatter plot of the centreline errors for 121 pairs of images that are successfully registered using EM and FCM (54 seeds) and (b) average errors in 10 percent range from 60–70 to 90–100.

TABLE II
COMPUTATION COMPLEXITY AND PERFORMANCE FOR EM AND FCM (150 SEEDS)

Methods	Pairs of images	Average centreline error (pixels)	Standard deviation (pixels)	Average time taken (s)
FCM	5	2.53	0.71	361.32
EM	5	2.76	0.69	117.75

model where the fast chamfer matching method is able to successfully register pairs of fundus images using small size of initial seeds set. The elastic matching algorithm outperforms the weak affine model based fast chamfer matching technique when there is a need for a larger number of initial seeds to search for global minimization.

REFERENCES

[1] D. E. Singer, D. M. Nathan, H. A. Fogel, and A. P. Schachar, "Screening for diabetic retinopathy," *Ann. Intern. Med.*, no. 116, pp. 660–671, 1992.

[2] J. B. A. Maintz and M. A. Viergever, "A survey of medical image registration," *Med. Image Anal.*, vol. 2, no. 1, pp. 1–36, 1998.

[3] C. Heneghan, P. Maguire, N. Ryan, and P. de Chazal, "Retinal image registration using control points," in *Proc. 2002 IEEE Int. Symp. Biomedical Imaging*, Jul. 2002, pp. 349–352.

[4] A. Can, C. V. Stewart, B. Roysam, and H. L. Tanenbaum, "A feature-based, robust, hierarchical algorithm for registering pairs of images of the curved human retina," *IEEE Trans. Pattern Anal/ Mach/ Intell/*, vol. 24, no. 3, pp. 347–364, Mar/ 2002.

[5] N. Ritter, R. Owens, J. Cooper, R. H. Eikelboom, and P. P. V. Saarloos, "Registration of stereo and temporal images of the retina," *IEEE Trans. Med/ Imag/.*, vol. 18, no. 5, pp. 404–418, May 1999.

[6] F. Zana and J. C. Klein, "A multimodal registration algorithm of eye fundus images using vessels detection and hough transform," *IEEE Trans. Med/ Imag/*, vol. 18, no. 5, pp. 419–428, May 1999.

[7] A. Pinz, S. Bernogger, P. Datlinger, and A. Kruger, "Mapping the human retina," *IEEE Trans. Med. Imag.*, vol. 17, no. 4, pp. 606–619, Aug. 1998.

[8] E. Peli, R. A. Augliere, and G. T. Timberlake, "Feature-based registration of retinal images," *IEEE Trans. Med. Imag.*, vol. 6, pp. 272–278, Sep. 1987.

[9] B. Fang, C. H. Leung, Y. Y. Tang, P. C. K. Kwok, K. W. Tse, and Y. K. Wong, "Offline signature verification with generated training samples," *Proc. Inst. Elect. Eng. (Vis., Image Signal Process.)*, vol. 149, no. 2, pp. 85–90, Apr. 2002.

[10] B. Fang, W. Hsu, and M. L. Lee, "Reconstruction of vascular structures in retinal images," in *Proc. ICIP'2003*, Barcelona, Spain, Sep. 2003, vol. 2, pp. 157–160.

[11] P. Jasiobedzki, "Registration of retinal images using adaptive adjacency graphs," in *Proc. 6th Annu. IEEE Symp. Computer-Based Medical Systems*, Jun. 1993, pp. 40–45.

[12] G. Borgefors, "Hierarchical chamfer matching: a parametric edge matching algorithm," *IEEE Trans. Pattern Anal. Mach. Intell.*, vol. 10, no. 6, pp. 849–865, Jun. 1988.

[13] O. Rockinger and T. Fechner, "Pixel-level image fusion: the case of image sequences," *Proc. SPIE (Signal Process., Sensor Fusion, Target Reco. VII)*, vol. 3374, pp. 378–388, 1998.

[14] C. V. Stewart, C.-L. Tsai, and B. Roysam, "The dual-bootstrap iterative closest point algorithm with application to retinal image registration," *IEEE Trans. Med. Imag.*, vol. 22, no. 11, pp. 1379–1394, Nov. 2003.

The Effect of the Cut Surface During Electrical Stimulation of a Cardiac Wedge Preparation

Bradley J. Roth*, Salil G. Patel, and Ryan A. Murdick

***Abstract*—Optical mapping from the cut surface of a "wedge preparation" allows observation inside the heart wall, below the epicardium or endocardium. We use numerical simulations based on the bidomain model to illustrate how the transmembrane potential is influenced by the cut surface. The distribution of transmembrane potential around a unipolar cathode depends on the fiber angle. For intermediate angles, hyperpolarization appears on only one side of the electrode, and is large and widespread.**

***Index Terms*—Bidomain, cardiac, electrical stimulation, fiber geometry, wedge preparation.**

I. INTRODUCTION

Optical mapping of the transmembrane potential is a common method for recording electrical activity in cardiac tissue [1]. One limitation of optical mapping is that it records the transmembrane potential from a thin layer on the surface of the heart. Often, researchers want to know what is happening deep in the heart wall. To overcome this limitation, several groups have begun to use a "wedge preparation" [2]–[5], which is prepared by slicing across the wall to create a cut surface. Optical mapping from this surface allows observation of the electrical behavior of regions inside the wall, below the epicardium and endocardium.

While a wedge preparation provides a unique view of what is happening deep inside the heart wall, it has limitations. Obviously, the tissue at the cut surface may be damaged. In this paper, we examine a subtler artifact inherent to these preparations. In a normal heart, the fiber geometry is complex with fiber direction rotating across the wall. At the epicardial and endocardial surfaces, the fibers are generally oriented in the plane of the surface. In a wedge preparation, however, fibers approach the cut surface at a variety of angles. We showed previously that if cardiac fibers approach an insulated surface at an angle, then an electrical shock can induce a surface transmembrane potential [6]. This polarization is caused by the cut surface, and would not be present had the heart wall been left intact.

We use numerical simulations to illustrate one example of how the transmembrane potential can be influenced dramatically by the cut surface during experiments using a wedge preparation. Our results indicate that studies of electrical stimulation (for example, defibrillation) must be interpreted cautiously.

II. METHODS

We use a passive bidomain model to represent the electrical behavior of cardiac tissue [7]. The fiber and electrode geometry are similar to that we have used previously [8]–[10] (Fig. 1). Circular electrodes of radius

Manuscript received November 18, 2004; revised July 17, 2005. This work was supported by in part the National Institutes of Heath (NIH) under research grant R01 HL57207, and in part by the American Heart Association—Midwest Affiliate. *Asterisk indicates corresponding author.*

*B. J. Roth is with the Department of Physics, Oakland University, Rochester, MI 48309-4487 USA (e-mail: roth@oakland.edu).

S. G. Patel is with the Department of Physics, Oakland University, Rochester, MI 48309-4487 USA.

R. A. Murdick is with the Department of Physics, Michigan State University, East Lansing, MI 48824 USA.

Digital Object Identifier 10.1109/TBME.2006.873386